atmosphere

MDPI

Article

Landfill Emissions of Methane Inferred from Unmanned Aerial Vehicle and Mobile Ground Measurements

Eduardo P. Olaguer [1,*], Shelley Jeltema [2], Thomas Gauthier [1], Dustin Jermalowicz [3], Arthur Ostaszewski [1], Stuart Batterman [4], Tian Xia [4], Julia Raneses [4], Michael Kovalchick [1], Scott Miller [1], Jorge Acevedo [1], Jonathan Lamb [1], Jeff Benya [1], April Wendling [1] and Joyce Zhu [1]

[1] Michigan Department of Environment, Great Lakes, and Energy, Lansing, MI 48909, USA; gauthiert@michigan.gov (T.G.); ostaszewskia@michigan.gov (A.O.); kovalchickm@michigan.gov (M.K.); millers@michigan.gov (S.M.); acevedoj1@michigan.gov (J.A.); lambj1@michigan.gov (J.L.); benyaj@michigan.gov (J.B.); wendlinga@michigan.gov (A.W.); zhuj@michigan.gov (J.Z.)
[2] Michigan Department of Technology, Management, and Budget, Lansing, MI 48909, USA; jeltemas@michigan.gov
[3] Cyber Felt Media Services, Midland, MI 48642, USA; info@cyberfelt.com
[4] School of Public Health, University of Michigan, Ann Arbor, MI 48109, USA; stuartb@umich.edu (S.B.); xiatian@umich.edu (T.X.); jraneses@umich.edu (J.R.)
* Correspondence: olaguerj@michigan.gov

Abstract: Municipal solid waste landfills are significant sources of atmospheric methane, the second most important greenhouse gas after carbon dioxide. Large emissions of methane from landfills contribute not only to global climate change, but also to local ozone formation due to the enhancement of radical chain lengths in atmospheric reactions of volatile organic compounds and nitrogen oxides. Several advanced techniques were deployed to measure methane emissions from two landfills in the Southeast Michigan ozone nonattainment area during the Michigan–Ontario Ozone Source Experiment (MOOSE). These techniques included mobile infrared cavity ringdown spectrometry, drone-mounted meteorological sensors and tunable diode laser spectrometry, estimation of total landfill emissions of methane based on flux plane measurements, and Gaussian plume inverse modeling of distributed methane emissions in the presence of complex landfill terrain. The total methane emissions measured at the two landfills were of the order of 500 kg/h, with an uncertainty of around 50%. The results indicate that both landfill active faces and leaking gas collection systems are important sources of methane emissions.

Keywords: methane; landfills; greenhouse gases; ozone precursors

Citation: Olaguer, E.P.; Jeltema, S.; Gauthier, T.; Jermalowicz, D.; Ostaszewski, A.; Batterman, S.; Xia, T.; Raneses, J.; Kovalchick, M.; Miller, S.; et al. Landfill Emissions of Methane Inferred from Unmanned Aerial Vehicle and Mobile Ground Measurements. *Atmosphere* **2022**, *13*, 983. https://doi.org/10.3390/atmos13060983

Academic Editor: Kostas Eleftheratos

Received: 31 May 2022
Accepted: 14 June 2022
Published: 18 June 2022

1. Introduction

Methane is the second most important greenhouse gas (GHG) after carbon dioxide [1,2]. According to the US Environmental Protection Agency (USEPA), Washington, DC, USA, municipal solid waste (MSW) landfills are the third-largest source of anthropogenic methane emissions in the United States, accounting for approximately 15.1 percent of these emissions in 2018 [3].

In addition to being a major GHG, methane is a tropospheric ozone precursor. Because of its low reactivity and long atmospheric lifetime compared to other organic precursors of ozone, the USEPA does not classify methane as a Volatile Organic Compound (VOC). However, recent studies by the State of California have shown that some landfills are "super-emitters" that may release up to 3000 kg/h of methane to the atmosphere [4,5]. Such releases of methane may significantly enhance radical chain lengths in atmospheric reactions of VOCs and nitrogen oxides that lead to local ozone formation. Olaguer [6] has shown, using an advanced microscale chemical transport model, that a large leak of landfill gas can create a significant addition to ambient ozone over large distances downwind. This

additional ozone is of the order of a few tenths of a part per billion (ppb) and is therefore non-negligible from the perspective of attaining the US National Ambient Air Quality Standard (NAAQS) for ozone, particularly in borderline ozone nonattainment areas such as Southeast Michigan (SEMI), where ozone design values (the three-year average of the annual fourth highest daily maximum eight-hour average ozone concentration measured at every monitoring station) for the three-year period of 2018–2020 exceeded the NAAQS by 1–2 ppb [7].

The State of Michigan has set a goal of achieving a 28 percent reduction below 1990 levels in GHG emissions by 2025 [8]. To achieve this goal, it is necessary to quantify current GHG emissions to better prioritize sources for controls, including MSW landfills. In addition, control of emissions of landfill gas may contribute to ozone attainment in SEMI. Assessment of the impacts of these controls may require more rigorous methods of landfill emissions estimation than the current practice of using the USEPA's LandGEM model [9].

The quantity of methane emitted by a landfill depends on the amount of organic waste that undergoes anaerobic microbial decomposition [10,11]. Other factors include the distribution and type of landfill cover [12], site-specific design features of the gas collection system, working practices, and daily/seasonal weather, including precipitation and especially barometric pressure [13]. Landfill temperature is also an important factor. Much attention has recently been devoted to Elevated Temperature Landfills (ETLFs), in which sub-surface temperatures rise beyond normal range due to biological and chemical reactions among waste products and the trapping of heat by liquids [14,15]. While this may suppress the methane content of landfill gas by exceeding the optimal range of temperatures for methane generation [16], physical deterioration of the gas collection system due to elevated temperatures may lead to fugitive emissions of methane.

Monster et al. [17] reviewed methodologies for measuring fugitive methane emissions from landfills. These methodologies included tracer gas dispersion, differential absorption LiDAR (DIAL), aerial measurements from aircraft, eddy covariance; static mass balance, and surface flux chambers. Shah et al. [18] summarized prior attempts to perform methane measurements by using Unmanned Aerial Vehicles (UAVs) and a variety of measurement techniques, including small, inexpensive sensors; tethered and on-board sampling; and fast, higher-precision instruments.

An international air-quality field study known as the Michigan–Ontario Ozone Source Experiment (MOOSE) [19] was conducted from May to September 2021, and one of its major sub-experiments was entitled Methane Releases from Landfills and Gas Lines (MERLIN). In this sub-experiment, the Michigan Department of Environment, Great Lakes, and Energy (EGLE) conducted a project to develop and test new methods for estimating landfill emissions of methane involving the operation of UAVs, otherwise known as drones. The main objectives of this project were (1) to demonstrate the feasibility of quantifying leaks of methane by using increasingly available drone-mounted sensors and other advanced instrumentation techniques and (2) to measure total and spatially distributed emissions of methane at two landfills in SEMI.

The larger of the two participating landfills is referred to here as Facility A, while the smaller landfill is referred to as Facility B. Part 115 of Michigan's Natural Resources and Environmental Protection Act (PA 451 of 1994 as amended) requires all landfills to report the amount of solid waste received annually [20]. In 2021, Facility A handled approximately 3 million cubic yards of municipal commercial and residential waste (MCW) and just under 1 million cubic yards of industrial (IW), construction and demolition (CD), and alternate daily cover (ADC) waste. (ADC is waste that may be used in lieu of soil as daily landfill cover.) Facility B processed around 800,000 cubic yards of MCW and 500,000 cubic yards of IW, CD, and ADC waste. Both Facility A and Facility B agreed to participate in MOOSE by allowing drone measurements to be conducted within and outside landfill boundaries.

2. Methodology

2.1. Measurement Platforms

The Scentroid DR1000 (Scentroid, 70 Innovator Ave Unit 7, Whitchurch-Stouffville, ON L4A 0Y2, Canada) is a UAV-mountable Flying Laboratory that contains up to five chemical sensors. When flown on a drone, the DR1000 can sample and analyze ambient air at heights of up to 150 m above ground level. For this project, a DR1000 was equipped with an LGD Compact-A (Axetris AG, Schwarzenbergstrasse 10, 6056 Kägiswil, Switzerland) Tunable Diode Laser Spectrometer (TDLS) with a methane lower detection limit of 0.4 ppm, at a sampling frequency of 2 Hz and a resolution of 10 ppb. In addition, the DR1000 carried a Global Positioning System (GPS) that was capable of concurrent reception of data from up to 3 Global Navigation Satellite Systems and an onboard pressure sensor to measure altitude. The DR1000 was mounted on a DJI M600 heavy lift drone. While in flight, the DR1000 recorded position, altitude, temperature, humidity, and ambient methane concentration. A Ground Station consisting of a specialized laptop with a high-gain WIFI antenna and Drone Information Management Software (DRIMS) allowed the user to control the Flying Laboratory and log all acquired data.

The quantification of landfill gas emissions requires measurements not only of ambient methane concentrations, but also of meteorological parameters such as the prevailing wind speed and direction, temperature, and pressure. A second drone was deployed to obtain these measurements, using a miniaturized anemometer. This was an Aegis IEV2 drone equipped with a BlueHalo WP-V2 UAS Weather Payload (BlueHalo, LLC, 410 Jan Davis Dr NW, Huntsville, AL 35806, USA), which measured and recorded the tilt, heading, and position of the drone in addition to meteorological parameters.

Fieldwork was conducted in the late summer of 2021, coinciding with the MOOSE campaign. This enabled drone measurements to be coordinated with ground-based mobile measurements based on infrared cavity ringdown (CRD) spectrometry by the University of Michigan, using the Michigan Pollution Assessment Laboratory (MPAL) [21]. The MPAL deployed two different CRD spectrometers (Picarro, 3105 Patrick Henry Dr., Santa Clara, CA 95054, USA), a Picarro G2401 and a Picarro G2204, which were mounted on the roof and at the front of the mobile lab, respectively. The MPAL was also equipped with meteorological instruments to measure wind speed, wind direction, temperature, and relative humidity in real time, as well as a GPS to mark locations of measurements.

2.2. Inverse Modeling of Methane Emissions

In typical US air-quality permit applications, the AERMOD Gaussian plume dispersion model [22] is used to compute ambient air concentrations around a facility given specified emissions at various facility release points. This is an example of "forward modeling". The opposite, known as "inverse modeling", infers emissions by means of a model that uses measured ambient air concentrations. For example, Lan et al. [23] used mobile lab measurements of atmospheric methane and an inverse Gaussian dispersion model based on AERMOD to quantify fugitive methane emissions from landfills and oil and natural gas operations in the Barnett Shale region of Texas.

Inverse modeling of ethylene oxide based on the Gaussian plume approximation was previously performed by EGLE for a medical sterilization facility in Grand Rapids, Michigan [24]. In that case, there was only a single source, and it enabled facility emissions of ethylene oxide to be estimated by using simple linear regression. Measurements of ethylene oxide were obtained from Summa canister samples that were analyzed by using gas chromatography with mass spectrometry detection (USEPA Method TO-15).

For this application, relevant aspects of AERMOD were re-coded in the Python language to construct a multilinear model in which an M $\times$ N matrix of transfer functions (describing the dispersion of methane plumes from N landfill point sources to M receptors in the presence of complex terrain) was multiplied by an N-dimensional column vector of methane emissions to yield an M-dimensional column vector of methane concentrations at receptors (measured by the front CRD spectrometer on the MPAL) minus the local back-

ground concentration (see below). Measured concentrations below a global background of 1.85 ppm were excluded in determining receptor concentrations or the local background concentration.

The inverse modeling problem is to infer the unknown emissions (the N-dimensional column vector) from the known receptor measurements (the M-dimensional column vector) and M × N transfer matrix. This was achieved by employing a multilinear equation solver for non-square coefficient matrices that is a standard mathematical optimization procedure. The Scipy algorithm, lsq_linear, was used as the numerical solver for this purpose. A similar method for landfill emissions estimation was demonstrated by Figueroa et al. [25], but without accounting for complex terrain.

The mathematical details of the transfer matrix and Gaussian plume dispersion parameters under both stable (evening through early morning) and convectively unstable conditions are described in the Supplementary Materials. The structure of the atmospheric boundary layer was accounted for by using standard AERMOD formulas. The height of the boundary layer (mixing height) and other dispersion parameters were inferred from available airport or site-specific meteorological data. In both the stable and convective cases, measurements of wind speed, wind direction, air temperature, and barometric pressure were required inputs, in addition to the roughness length (set at 0.1 m) and cloud cover (based on nearby airport indications). Additional required inputs in the convective case included the surface albedo (set at 0.23) and the Bowen ratio (set at 0.55). These surface parameters were estimated for local Michigan conditions, using the USEPA's AERSURFACE preprocessor [26].

A horizontal domain was determined for modeling purposes that included the entire landfill property and enough of the surrounding area to encompass measurements conducted during the period of interest. Figures 1 and 2 show approximate model domains for the two surveyed landfills, along with contours of terrain elevation above the local background elevation. The terrain beyond landfill boundaries is very flat. Ambient air measurements and potential source locations were assigned to grid cells within the model domain. If there were multiple measurements within a receptor grid cell, then the average of the measurements was used as the receptor concentration. A horizontal grid resolution of 100 m was sufficient in the case of Facility A. In the case of Facility B, a finer resolution of 10 m was warranted. Due to this finer resolution, variations in elevation were accounted for only within the landfill in the case of Facility B. In both cases, the vertical domain had a grid resolution of 10 m with the model top at 800 m.

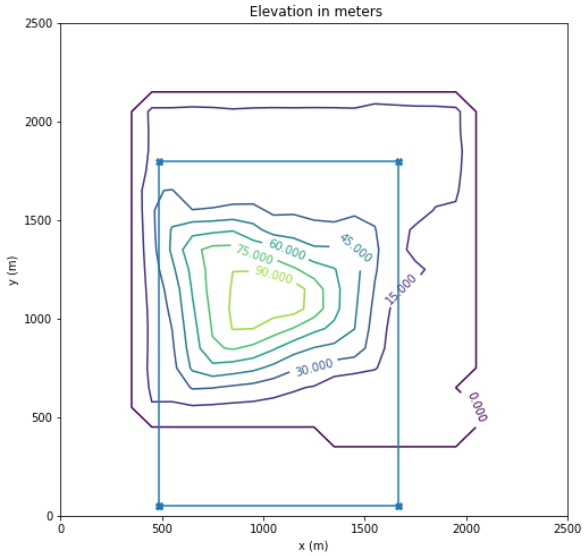

Figure 1. Model domain and terrain elevation above local background for Facility A. Blue line is approximate border of the landfill.

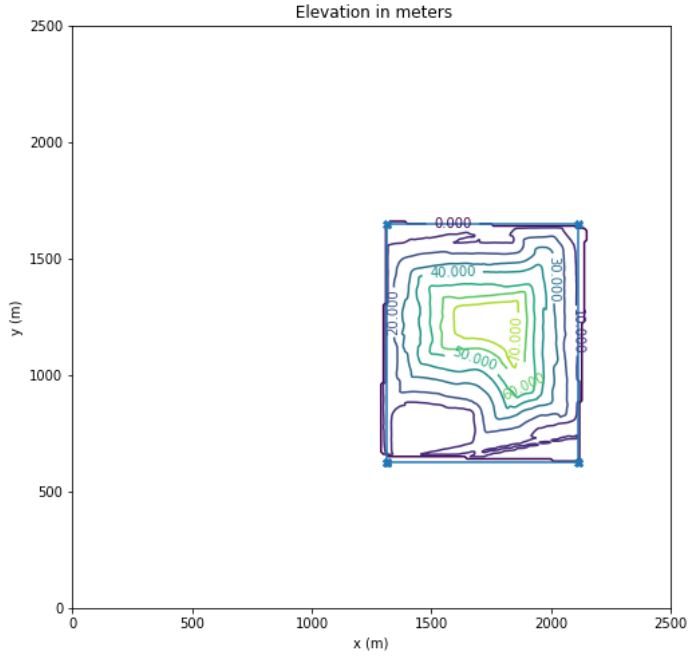

Figure 2. Model domain and terrain elevation above local background for Facility B. Blue line is approximate border of the landfill.

Among the important parameters required by the inverse model is the local background methane concentration. To compute this quantity, the model first identified the measurement receptors that were not downwind of any plausible emission sources within the landfill based on the transfer matrix. The average of all the upwind measurements was then computed and compared to the minimum downwind methane concentration. The smaller of these two values was then assigned as the local background concentration. This accommodated the possibility that the upwind concentrations were the result of landfill air recirculation, especially in the case of a stable boundary layer. It also guaranteed that the receptor column vector included only positive values.

If unconstrained, the inverse model described above can assign emissions to various grid cells within the landfill in such a way as to grossly overestimate the total emissions of methane. This may be related to the degree to which the linear system is underdetermined due to the mismatch between the number of release points and the number of receptors. To avoid this problem, total emissions were specified as a model constraint, implemented by adding a row to the transfer matrix with each element assigned a value of 1, and adding a row to the receptor column vector with a single element set equal to the constrained total emissions. The total methane emission rate was therefore treated as a parameter that could be inferred from the performance statistics of various emission scenarios. A linear regression of measured versus simulated methane concentrations at the receptor grid cells was computed for each emission scenario. The inferred total methane emission rate was obtained from the scenario that yielded values of the regression slope and correlation coefficient closest to 1.

2.3. Model Inversions of Mobile Laboratory Data

During the early phase of MOOSE, prior to the deployment of the EGLE drone systems, the MPAL visited various landfills in SEMI to perform methane characterization experiments. What follows is a demonstration of the inverse model technique at 100 m cell resolution based on mobile lab data collected at Facility A on 5 June 2021, during which cloud cover was estimated at 50% throughout the morning.

Figure 3 shows MPAL measurements of methane concentration outside the landfill from 7:10 a.m. to 7:27 a.m. that day. The inferred local background concentration was 2.0 ppm. Based on MPAL meteorological measurements, the vector-averaged wind during

that period was 1.8 m/s from a direction of 246° (southwesterly). The average temperature and barometric pressure were 294.5 K and 979 mb, respectively. The inferred mixing height under stable conditions was 136 m.

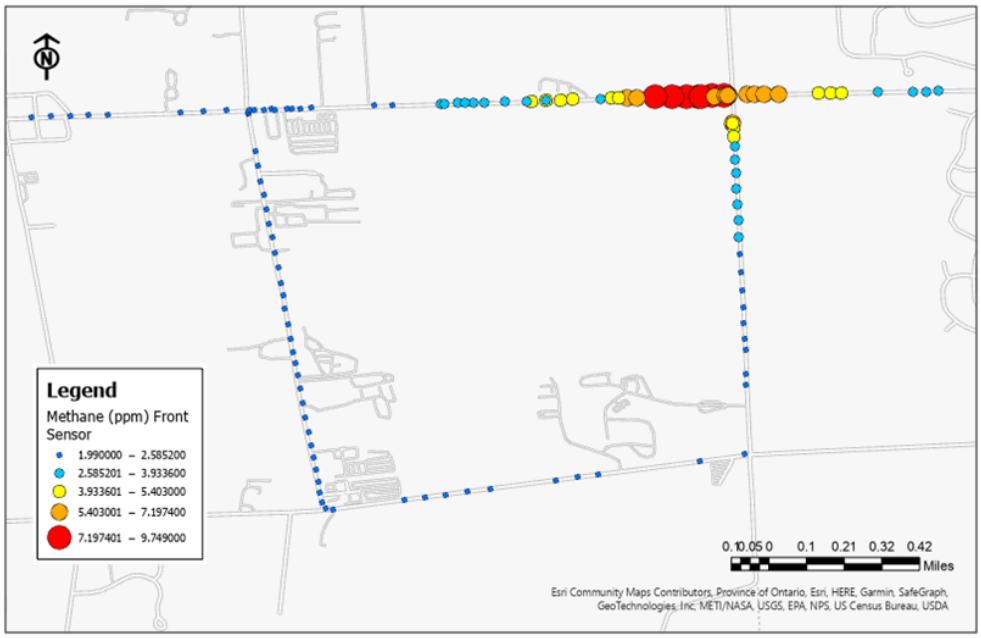

Figure 3. CH_4 concentrations (ppm) measured by MPAL on 5 June 2021, 7:10 a.m. to 7:27 a.m.

The best model performance was obtained when total emissions were set to 500 kg/h. This is illustrated by Figure 4, which plots measured concentrations versus concentrations at the receptor sites predicted by the forward model based on emissions inferred by the inverse model. Figure 4 also shows the slope and correlation coefficient (R) obtained from linear regression, both of which are close to 1.

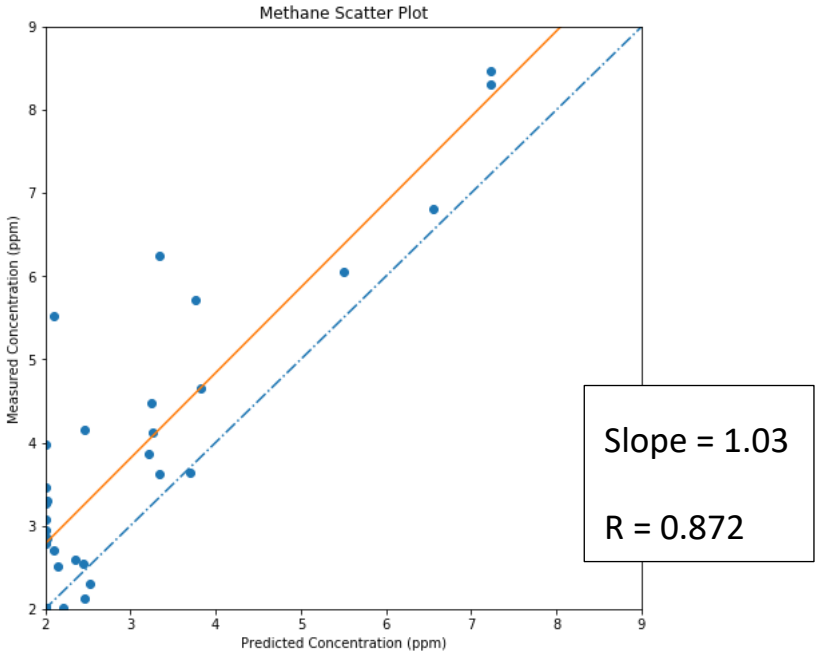

Figure 4. Scatter plot of measured methane concentrations versus modeled concentrations for 5 June 2021, 7:10 a.m. to 7:27 a.m. R denotes the correlation coefficient. The (orange) regression and (blue) 1:1 lines are also displayed.

Figure 5 shows the spatial distribution of landfill emissions of methane inferred by the inverse model from the MPAL measurements. The inferred emissions arise mainly from areas around gas wells located at the northern end of the landfill. The presence of these leaks was confirmed by Surface Emission Monitoring (SEM) conducted by EGLE inspectors, using a handheld Non-Dispersive Infrared (NDIR) methane sensor. Leaks on the northeastern side were due to the removal of gas wells in preparation for a new waste cell, while those in the northwest were due to flooded wells and insufficient cover in an area of high methane production associated with relatively new waste.

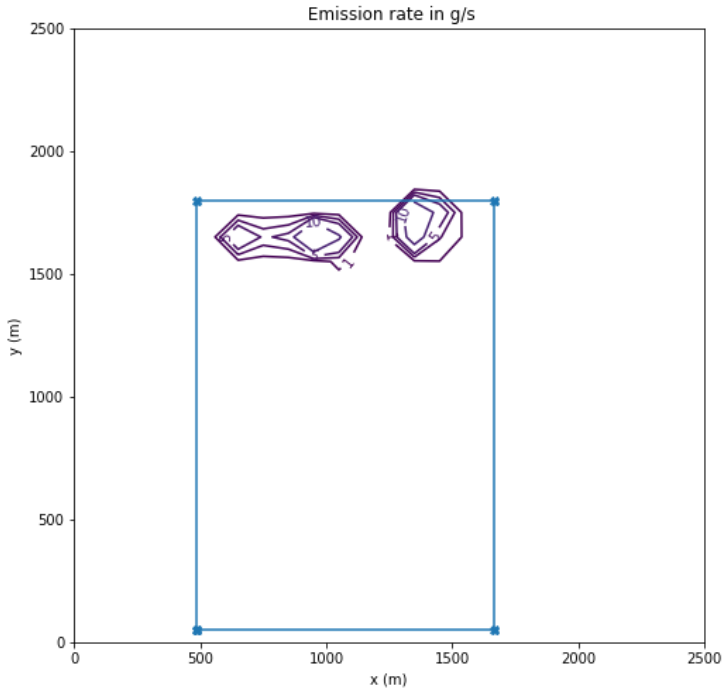

Figure 5. Inferred distribution of landfill emissions of methane for 5 June 2021, 7:10 a.m. to 7:27 a.m., based on MPAL measurements. Contours are drawn for 1, 3, 5, and 10 g/s. Blue line is approximate border of the landfill.

Figures 6–8 display similar information as Figures 3–5 but using MPAL measurements conducted at Facility A from 10:24 a.m. to 10:39 a.m. on 5 June 2021. The corresponding local background methane concentration was 1.98 ppm. The vector-averaged wind during that period was 3.1 m/s from a direction of 246° (southwesterly). The average temperature and pressure were 299 K and 980 mb, respectively. The inferred mixing height under convective conditions was 431 m. The inferred emissions for the late morning were also 500 kg/h, which is consistent with the median methane emissions reported in the California Methane Study, but below the high end (>1000 kg/h) of super-emitting landfills [4,5]. Note that the inferred emissions are again at the northern edge of the landfill, rather than in the landfill interior.

A portion of landfill methane emissions may come from the active face and associated side slopes of the landfill that are often significantly elevated in height compared to gas wells near the facility fence line. Plumes from this part of the landfill may not have been sensed by the MPAL, owing to their elevation. Moreover, the inverse model is very sensitive to the assumed total emissions of methane. A direct measurement of total emissions is therefore highly desirable to increase confidence in the inverse model results.

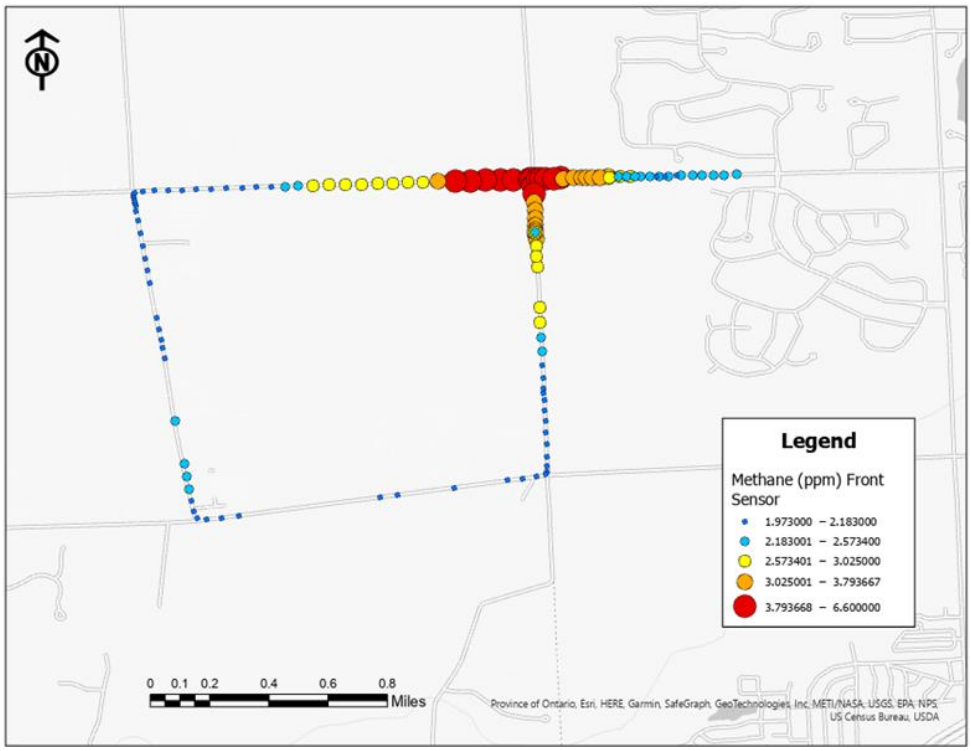

Figure 6. CH_4 concentrations (ppm) measured by MPAL on 5 June 2021, 10:24 a.m. to 10:39 a.m.

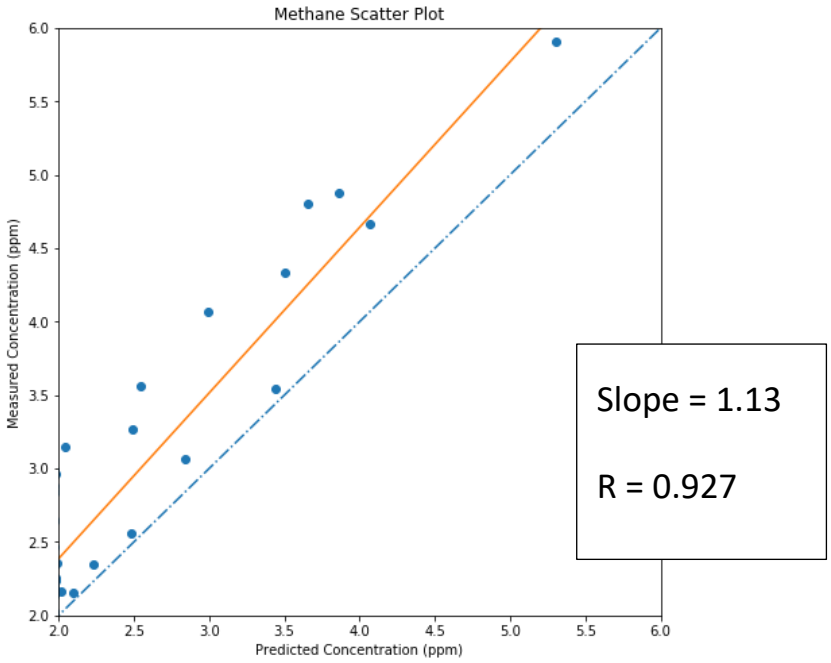

Figure 7. Scatter plot of measured methane concentrations versus modeled concentrations for 5 June 2021, 10:24 a.m. to 10:39 a.m. R denotes the correlation coefficient. The (orange) regression and (blue) 1:1 lines are also displayed.

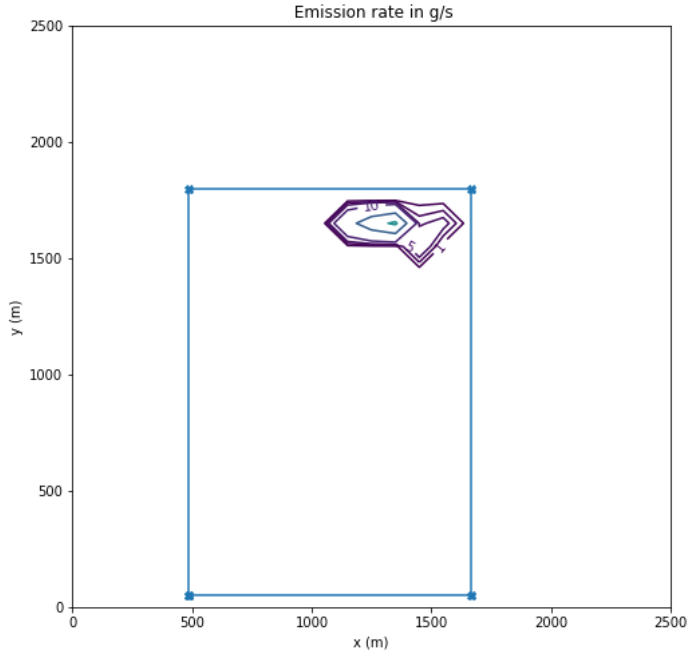

Figure 8. Inferred distribution of landfill emissions of methane for 5 June 2021, 10:24 a.m. to 10:39 a.m., based on MPAL measurements. Contours are drawn for 1, 3, 5, 10, 30, and 50 g/s. Blue line is approximate border of the landfill.

2.4. Drone Measurement Strategy

The limitations described in the previous paragraph were a strong motivation to deploy drone-mounted sensors. The drone measurement strategy consisted of two parts: (1) estimation of the total landfill emissions by measuring horizontal methane fluxes through a vertical plane (flux plane) and (2) raster grid measurements directly above interior landfill sources.

A Python code was developed to enable methane fluxes to be calculated. The algorithm divided the flight interval of a drone into vertical bins (typical width of ~10 m) for which the bin averages of various parameters were computed, including the vector wind, the excess methane concentration above a global background of 1.85 ppm, and the atmospheric density. The assumption in the calculation is that sources within the landfill predominantly contribute to the excess methane over background. (The global background was used as a threshold rather than the local background to maintain independence from other measurements.) Moreover, only the flux component perpendicular to the chosen flux plane was counted, so that the total methane flux for the landfill was the sum of positive fluxes minus the sum of negative fluxes for all distinct flux planes.

The flux plane method described above differs from the near-field Gaussian plume inversion flux quantification method of Shah et al. [18,27] in that the former method is applied downwind of an entire collection of landfill sources. The method of Shah et al., however, focuses on upwind and downwind flux measurements, using drones flying very near single point sources.

The two participating landfills provided staff to assist EGLE personnel in the planning and implementation of the drone flights during the project. As part of the standard pre-flight procedures, the Pilot in Command (PiC) checked the ground wind directions on multiple flight applications and coordinated with landfill staff to find the optimal locations for perpendicular flux plane and raster grid patterns. Minimizing the interference from truck traffic, as well as staying away from the actual working area of the landfill, sometimes resulted in less-than-optimal flight patterns or locations.

The typical flux plane flight was downwind from the active face of the landfill. The take-off/landing area was located so as not to interfere with landfill operations and yield the longest straight flight path. The DR1000 would climb to 10 m above ground level

after takeoff, fly until it reached the end of the straight line or reached an obstruction, ascend 10 m, and then fly back. This pattern would be repeated until methane levels fell to back down to background levels or the carrying drone reached the US Federal Aviation Administration (Washington, DC, USA) maximum ceiling (allowed height), after which the drone returned to the landing area. The heights of many flights peaked at around 40 m above ground level.

The typical raster flight started from the same takeoff/landing site as the flux plane flight and was oriented perpendicular to the wind. The PiC and the landfill team would estimate the flight altitude needed to cover the raster area. This ranged from 20 to 50 m above perimeter elevation depending on any obstructions. Once the DR1000 was at the correct altitude, the PiC would fly the drone to the far end of the area of interest. The drone would be kept at the same altitude, but it would be flown 10 m toward the landfill surface and then start its return trip. This would be repeated until the drone reached a height of 10 m above the surface. From there, the PiC would start flying segments that were as close to perpendicular to the previous flight paths, again maintaining a constant altitude and 10 m spacing between flight segments. The drone would return to the landing area as soon as it reached the end of the area or an obstruction that prevented it from completing the ideal pattern.

The Aegis meteorological platform was flown primarily in a vertical pattern at a location that best represented the vertical wind profile pertaining to the Scentroid DR1000 flight plan of interest. Flight segments for both drone platforms were based on visual observations due to the day-to-day changes at the landfills. Because the Aegis did not always fly with the compass pointed in the direction of magnetic north, a correction factor was applied to the measured wind direction. The ground course readings from the flight logs were verified with the actual flight recording showing the compass direction and then averaged to produce the appropriate correction factor.

3. Results of Drone Monitoring

3.1. Facility A on 14 September 2021

An example of the potential effectiveness of drone measurements is provided by an analysis of data collected at Facility A on 14 September 2021, from 9:04 a.m. to 9:23 a.m. (The MPAL was not present at the landfill that day.) Unfortunately, an electrical problem with the meteorological platform wiped out all the data on the Secure Digital (SD) card, so instead of direct wind measurements, this analysis makes use of nearby airport data supplemented by vertical extrapolations of the wind measurement at anemometer level to other heights based on standard AERMOD formulas. The airport anemometer level wind speed and wind direction were 5.36 m/s and 200°, respectively, while the air temperature was 295 K. Cloud cover was estimated at 70%. The resulting inferred mixing height was 790 m.

Figure 9 shows flux plane data collected at the downwind edge of the landfill. Note that, despite the very high mixing height, the fence line methane concentrations are often well above 10 ppm. The calculated outgoing methane flux in this case was 555 kg/h.

Figure 10 shows raster measurements in the interior of Facility A. The local background methane concentration inferred from the raster measurements was 2.05 ppm. Figure 11 shows the solution quality of an inverse model run with only drone raster data as input, at a 100 m cell resolution, and with total methane emissions of 555 kg/h. The solution quality is acceptable ($R^2 > 0.5$) without any tuning of model parameters.

Figure 12 shows the distribution of landfill emissions of methane obtained from the drone measurements, which now include elevated emissions on the active face of the landfill, as well as emissions from sources further downwind until the edge of the landfill. The leak locations inferred from the drone measurements were once more verified by SEM measurements conducted by EGLE inspectors, using a handheld NDIR methane sensor.

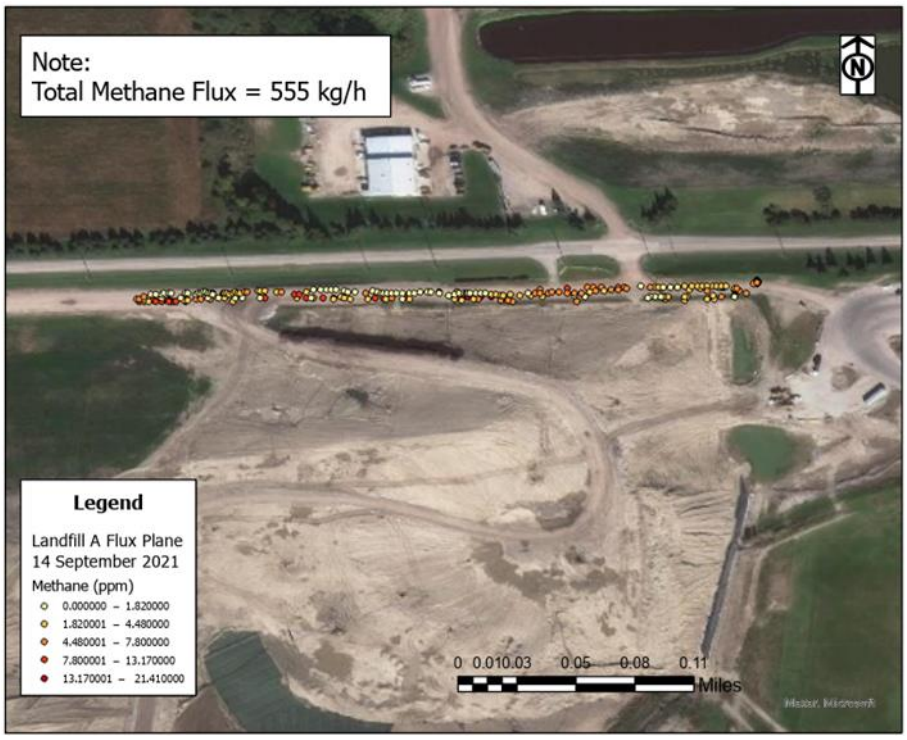

Figure 9. Methane concentrations measured at the downwind edge of Facility A on 14 September 2021, 9:04 a.m. to 9:23 a.m. The height of the flux plane was 35 m.

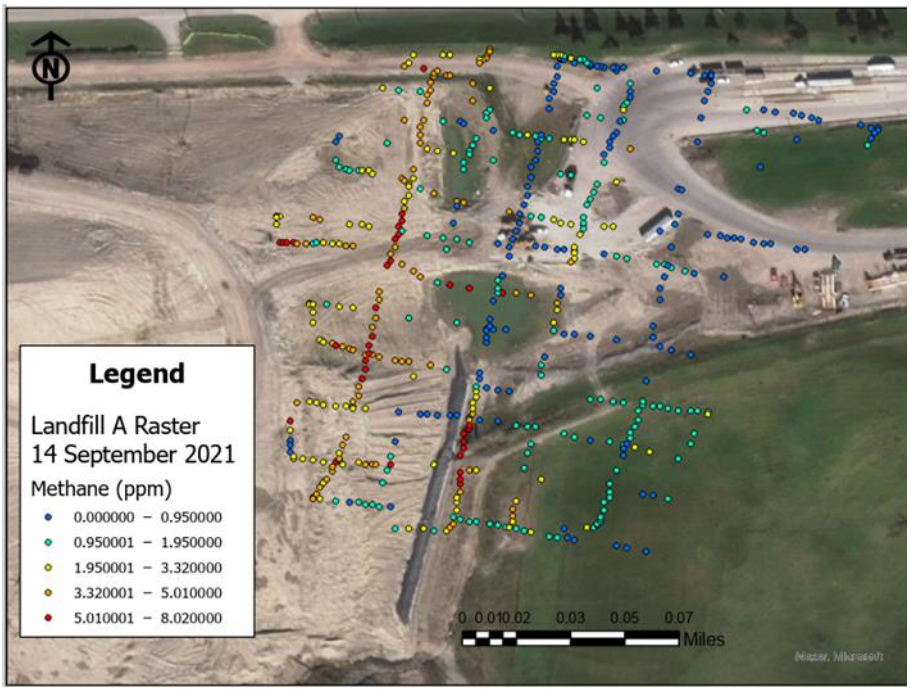

Figure 10. Methane concentrations measured in the interior of Facility A on 14 September 2021, 9:04 a.m. to 9:23 a.m. The maximum altitude of measurements was roughly 40 m above the set point.

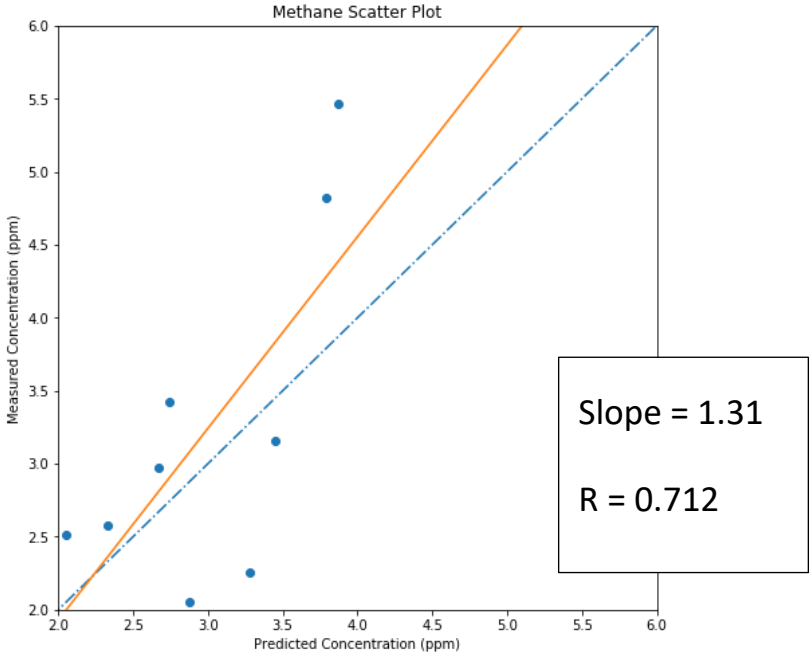

Figure 11. Scatter plot of measured methane concentrations versus modeled concentrations for 14 September 2021, 9:04 a.m. to 9:23 a.m. R denotes the correlation coefficient. The (orange) regression and (blue) 1:1 lines are also displayed.

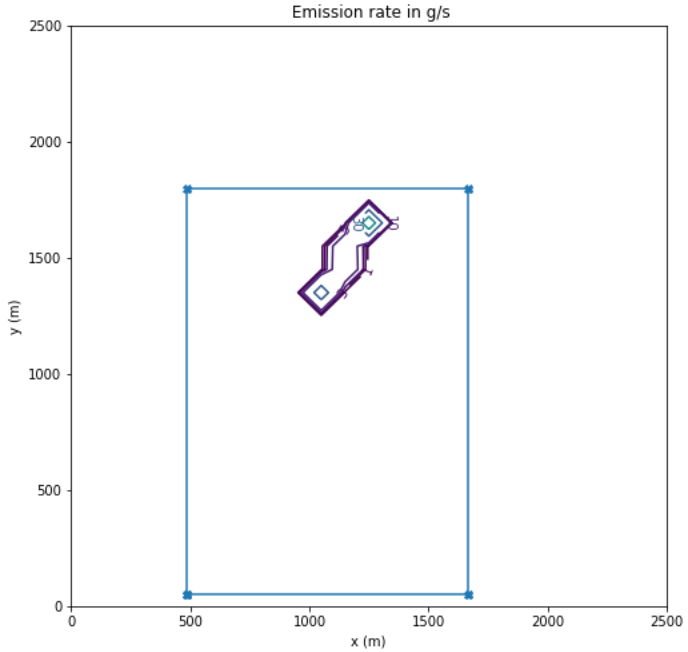

Figure 12. Inferred distribution of landfill emissions of methane on 14 September 2021, 9:04 a.m. to 9:23 a.m., based on drone measurements. Contours are drawn for 1, 3, 5, 10, 30, and 50 g/s. Blue line is approximate border of the landfill.

3.2. Facility B on 28 September 2021

The only day on which the Aegis meteorological platform was successfully deployed to enable a flux plane evaluation to be conducted with local wind measurements, as well as the DR1000′s methane sensor, was 28 September 2021. The MPAL was also present on September 28 and was able to conduct mobile CRD measurements around the perimeter of Facility B, as shown in Figure 13.

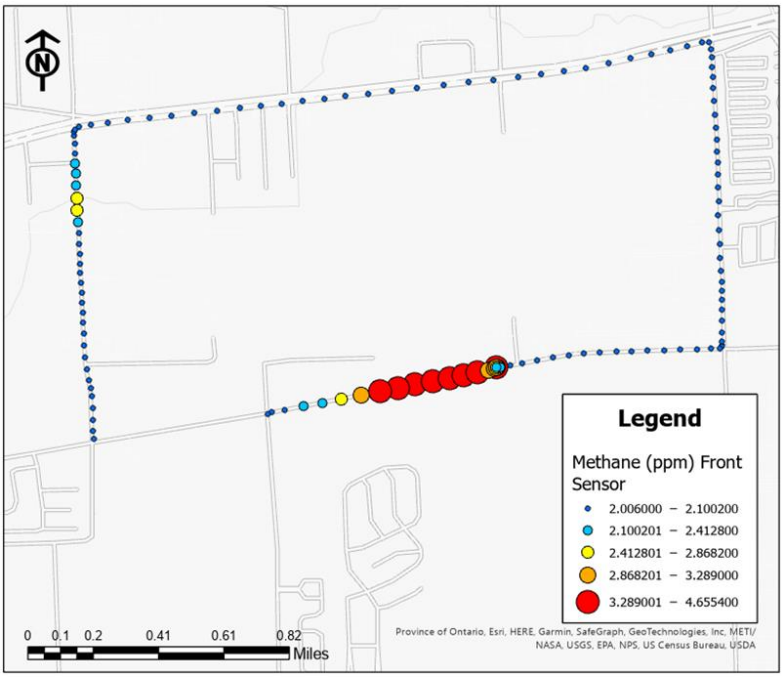

Figure 13. CH_4 concentrations (ppm) measured by MPAL on 28 September 2021, 9:01 a.m. to 9:22 a.m.

The wind measured by the MPAL during the period of interest was close to calm (~1 m/s), and so the MPAL could not be relied on to provide a stable wind direction. The nearest airport reported anemometer-level winds of 10 mph (=4.47 m/s) from the direction of north northeast (NNE).

Facility B is a heavily screened landfill, with buildings, power lines, main roads, and other obstacles to drone flights located on its perimeter. This made it very difficult to conduct flux plane measurements immediately outside the landfill. Interference of built structures with the wind flow may also explain why the MPAL measured relatively calm winds at ground level around the landfill. Based on the prevailing northeasterly wind direction and ongoing landfill activities, the project team decided to conduct flux plane measurements at an elevated area in the vicinity of the active face of the landfill.

Figures 14 and 15 show two sets of flux plane measurements with the DR1000. The first set, referred to as the Western Flux Plane, consists of a relatively shallow flight plane that is supplemented by a deeper flight plane at the summit of the active face above the first flight plane. The total depth of the Western Flux Plane was about 36 m. The second set, referred to as the Southern Flux Plane, was conducted at the southern edge of the active face with a total flight depth of 23 m. A vertical meteorological profile was conducted separately for each DR1000 flux plane set. The computed methane fluxes were 233.9 kg/h for the Western Flux Plane, and 203.5 kg/h for the Southern Flux Plane. The total estimated methane emissions from the landfill were, thus, 437 kg/h.

Note that the Carbon Mapper Global Observatory [28] made aircraft measurements on a separate date for Facility B, which indicated a 227 kg/h plume from the active face of the landfill. Although day-to-day variability is only one component of uncertainty in fugitive emissions of methane, the difference between the Carbon Mapper measurement and the drone-based measurement suggests an uncertainty of about 48%.

In addition to the flux plane measurements, the DR1000 was flown in a raster pattern directly over the active face of the landfill, as illustrated in Figure 16. The local background methane concentration inferred from the combination of DR1000 and MPAL measurements was 2.0 ppm.

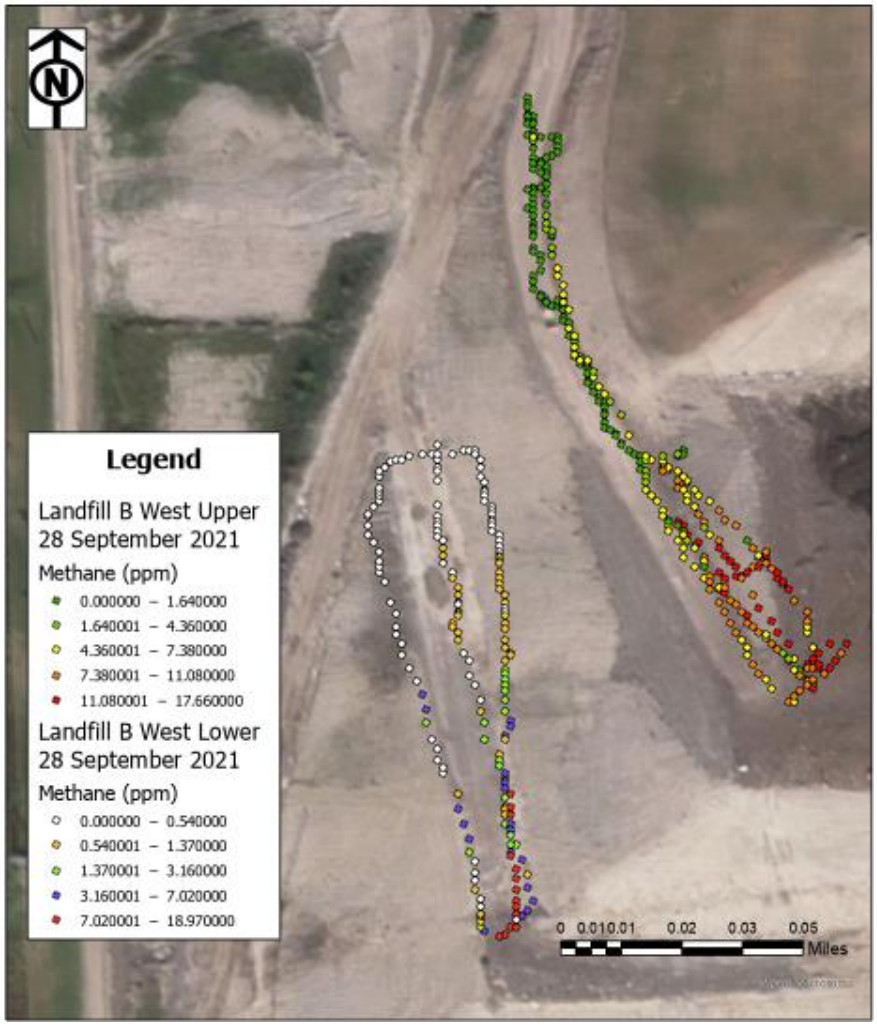

Figure 14. DR1000 measurements of methane for the Western Flux Plane at Facility B on 28 September 2021.

The MPAL and drone (both flux plane and raster) measurements were fed to the Gaussian plume inverse model constrained by total methane emissions of 437 kg/h. The model anemometer wind speed was set at the lowest value measured by the Aegis platform, namely 3 m/s. The corresponding wind direction was set at 36 degrees, which was the closest direction to NNE measured by the Aegis platform. Both the wind speed and wind direction selected for the inverse model were associated with the lowest layer in the Southern Flux Plane. These parameter choices were made to be as consistent as possible with the anemometer wind speed and direction reported at the nearest airport, while still reflecting local wind measurements. Additional model input parameters included surface temperature and pressure values of 290 K and 990 mb inferred from MPAL measurements, and a cloud cover of 30% based on airport conditions. A convective boundary layer height of 385 m was inferred for this case.

Figure 17 displays the scatter plot for the case of 28 September 2021 at Facility B. Once more, the solution quality is acceptable ($R^2 > 0.5$), without any tuning of model parameters. The lower correlation coefficient relative to the cases of 5 June probably reflects the wind variability observed by the MPAL during the morning of 28 September.

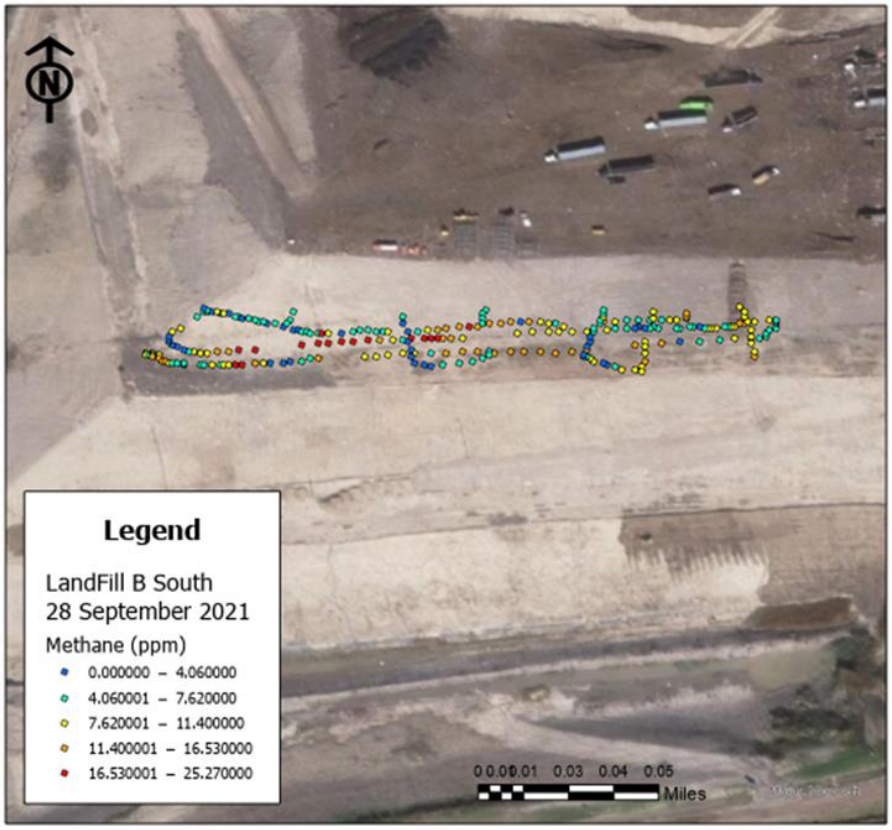

Figure 15. DR1000 measurements of methane for the Southern Flux Plane at Facility B on 28 September 2021.

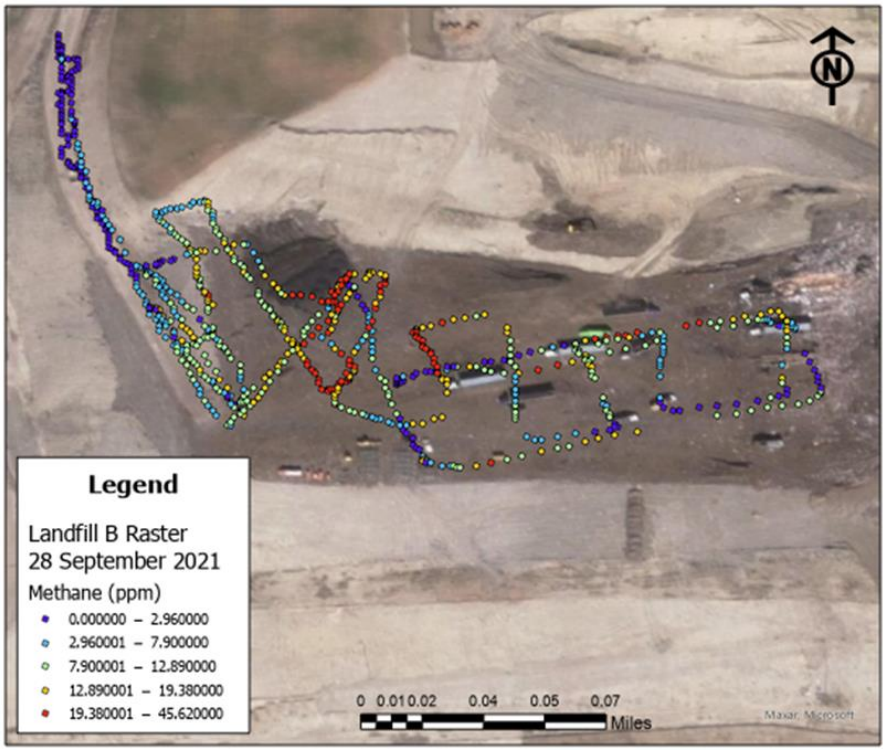

Figure 16. DR1000 raster measurements of methane at Facility B on 28 September 2021. The maximum altitude of the measurements was roughly 28 m above the set point.

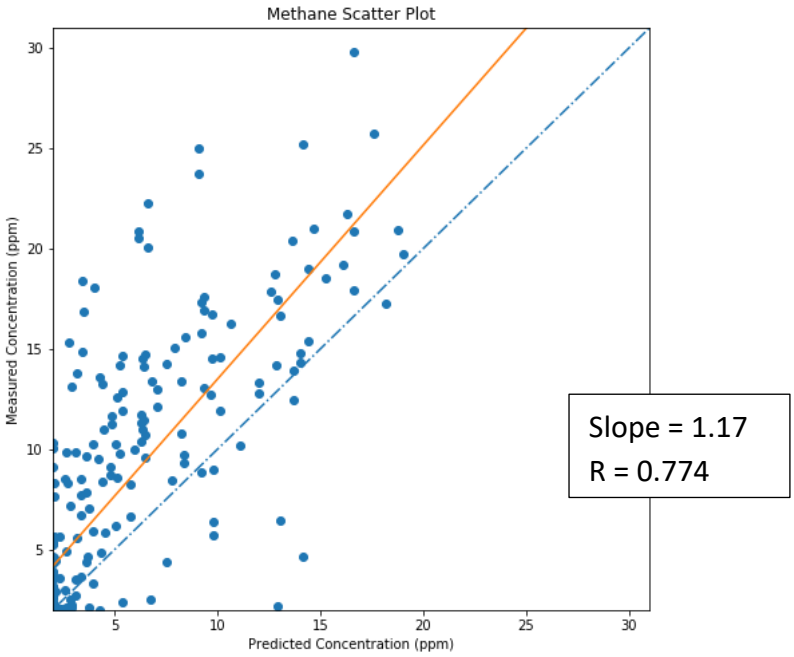

Figure 17. Scatter plot of measured methane concentrations versus modeled concentrations for 28 September 2021, 9:01 a.m. to 9:54 a.m. R denotes the correlation coefficient. The (orange) regression and (blue) 1:1 lines are also displayed.

Figure 18 shows the locations of highest emissions within the landfill deduced from the inverse model. These emissions were clustered in the active face, as confirmed by SEM monitoring by EGLE inspectors on the same day. The maximum localized (point source) emission rate inferred by the inverse model was 10.5 g/s.

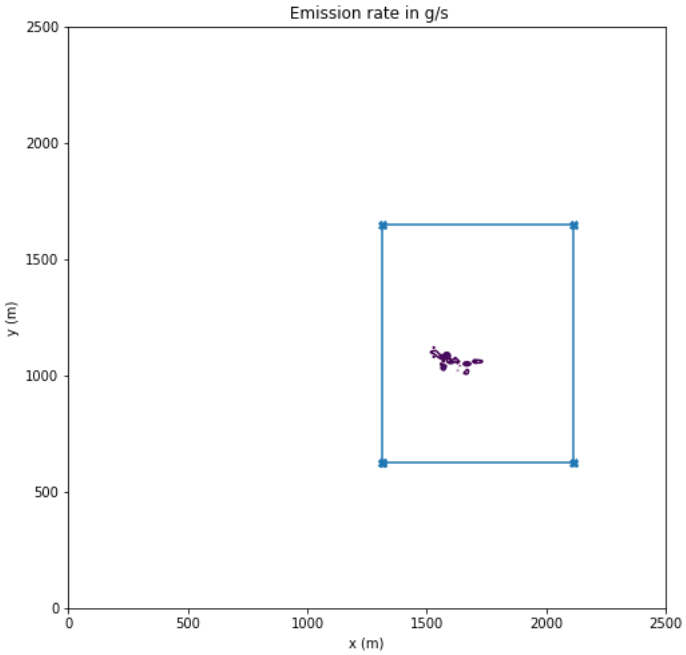

Figure 18. Inferred distribution of landfill emissions of methane on 28 September 2021, 9:01 a.m. to 9:54 a.m., based on drone and MPAL measurements. Contours are drawn for 1, 3, 5, and 10 g/s. Blue line is approximate border of the landfill.

4. Discussion and Conclusions

This project successfully deployed several advanced techniques to measure methane and estimate emissions from two landfills in the SEMI ozone nonattainment area during the MOOSE field study. These techniques included the following:

- Mobile infrared cavity ringdown spectrometry;
- Drone-mounted tunable diode laser spectrometry;
- Drone-mounted meteorological sensors;
- Estimation of total emissions of methane based on flux plane measurements;
- Gaussian plume inverse modeling of distributed methane emissions.

The results indicated that emissions from both the active face of the landfill and leaking gas collection systems are important sources of landfill emissions. This is an important finding because reported methane emissions from landfills typically do not account for contributions from the active face. Consequently, GHG-emission inventories may significantly understate the role that landfills play in climate change.

The total methane emissions measured at the two participating landfills were of the order of 500 kg/h, significantly lower than the upper range of emissions reported in the California Methane Study. In the case of Facility A, the lower emission rate is likely due to significant improvement in work practices resulting from a change in ownership before the MOOSE campaign, as noted by EGLE inspectors.

The results of this study may be compared to the landfill total methane emission rates measured by Lan et al. [23] for four landfills in the Barnett Shale region, which ranged from 86 to 2087 kg/h, with an average total emission rate of 738 kg/h. Comparing this average value with the MOOSE drone measurements suggests that the uncertainty in the drone-based estimates is of the order of 50%, similar to the uncertainty estimate derived from a comparison with Carbon Mapper. This is within the lower and upper uncertainty bounds of 17% and 227% estimated by Shah et al. [27] for their drone flux measurements. Galfalk et al. [29] also used drones to perform multiple methane flux plane measurements surrounding a sludge pile at a wastewater treatment plant with higher resolution wind measurements than in this study. Their reported uncertainties were around 6%, suggesting that spatial and temporal variability are larger sources of emissions uncertainty than measurement error. More recently, Corbett and Smith [30] employed a tunable diode laser on both fixed-wing and multi-rotor UAVs to estimate the uncertainty of methane emissions measurements based on controlled release experiments, as well as real field data. For their quadcopter rotary drone surveys, they estimated errors of less than 32% absolute difference and 24.8% average difference when flying downwind flux planes.

The limited scenarios considered here only partially address the considerable variability in landfill emissions indicated by mobile lab data from the entire MOOSE campaign, which will be the subject of a separate paper. Because of limited success in the deployment of the Aegis drone measurement platform and other technical problems that arose during the project, a larger set of directly measured total methane fluxes using the drone technique could not be provided. More studies are warranted to better characterize and quantify the variability of landfill gas emissions and the factors that contribute to it.

The novelty of this research is that this is the first application of drone measurements and an inverse model to infer both total and distributed emissions of methane from an entire landfill in the presence of complex terrain, in contrast to the prior studies of Figueroa et al. [25] and Shah et al. [27]. Ali et al. [31] applied a Gaussian plume model and the stochastic optimization technique of Kormi et al. [32] to perform inverse modeling of methane emissions from a landfill in Georgia based on a combination of SEM, drone, and downwind mobile lab measurements. However, their inverse model did not account for complex terrain and employed simpler estimates of dispersion based on the Briggs method [33]. The technique described in this study is highly efficient and can provide results in near-real time, that is within a few hours after measurements are completed. Possible future extensions of this research may involve drone-enabled tomographic measurements

based on open-path optical instruments, such as the ground-based tomographic network demonstrated by Olaguer et al. [34].

The benefits of this research include an increased ability to locate and quantify methane emissions, not only from landfills, but from other sources as well, such as oil and gas exploration and production and waste management facilities. Improved methane emission inventories will enable countries to better identify appropriate emission control strategies and live up to their agreement under the Glasgow Conference of Parties in November 2021 (COP26) to reduce methane emissions by 30 per cent by 2030 compared to 2020 levels [35]. Moreover, it will enable national, state, and local regulators to reduce exposure to ground-level ozone by reducing emissions of methane, as well as accompanying VOCs, especially through real-time leak detection and repair (LDAR).

Supplementary Materials: The following supporting information can be downloaded at: https://www.mdpi.com/article/10.3390/atmos13060983/s1, Gaussian Plume Formulation.

Author Contributions: Conceptualization, E.P.O.; methodology, E.P.O., S.J. and S.B.; software, E.P.O. and S.J.; validation, M.K., J.A., J.L. and J.B.; formal analysis, E.P.O.; investigation, E.P.O., S.J., T.G., D.J., A.O., S.B., T.X. and J.R.; resources, S.M., A.W. and J.Z.; data curation, S.J. and J.R.; writing—original draft preparation, E.P.O. and S.J.; writing—review and editing, S.B.; visualization, S.J.; supervision, S.J., D.J., S.M. and A.W.; project administration, E.P.O.; funding acquisition, E.P.O. All authors have read and agreed to the published version of the manuscript.

Funding: This research was funded by the US Environmental Protection Agency, Washington, DC, USA, grant number XA00E02952; and by the US Department of Energy, Washington, DC, CFDA # 81.041, State Energy Program.

Institutional Review Board Statement: Not applicable.

Informed Consent Statement: Not applicable.

Data Availability Statement: Related data for this study and other components of MOOSE can be found at https://www-air.larc.nasa.gov/missions/moose/index.html (accessed on 30 May 2022).

Acknowledgments: We would like to acknowledge Brandy Brown and Robert Jackson of Michigan EGLE for their support in obtaining US Department of Energy funding for this project.

Conflicts of Interest: The authors declare no conflict of interest.

References

1. Stocker, T.F.; Qin, D.; Plattner, G.-K.; Tignor, M.; Allen, S.K.; Boschung, J.; Nauels, A.; Xia, Y.; Bex, V.; Midgley, P.M. Intergovernmental panel on climate change (IPCC). In *Climate Change 2013: The Physical Science Basis. Contribution of Working Group I to the Fifth Assessment Report of the Intergovernmental Panel on Climate Change*; Cambridge University Press: Cambridge, UK; New York, NY, USA, 2013.
2. Zhang, J.; Han, G.; Mao, H.; Pei, Z.; Ma, X.; Jia, W.; Gong, W. The spatial and temporal distribution patterns of XCH4 in China: New observations from TROPOMI. *Atmosphere* **2022**, *13*, 177. [CrossRef]
3. U.S. Environmental Protection Agency. Basic Information about Landfill Gas. Available online: https://www.epa.gov/lmop/basic-information-about-landfill-gas#methane (accessed on 25 January 2022).
4. Duren, R.; Thorpe, A.; Foster, K.T.; Rafiq, T.; Hopkins, F.M.; Yadav, V.; Bue, B.; Thompson, D.R.; Conley, S.; Colombi, N.; et al. California's methane super-emitters. *Nature* **2019**, *575*, 180–184. [CrossRef] [PubMed]
5. Duren, R.; Thorpe, A.; McCubbin, I. *The California Methane Survey*; CEC-500-2020-047; California Energy Commission: Sacramento, CA, USA, 2020.
6. Olaguer, E.P. The potential ozone impacts of landfills. *Atmosphere* **2021**, *12*, 877. [CrossRef]
7. State of Michigan. Monitoring Data for Violating Monitors in Nonattainment Areas (2018–2020). Available online: https://www.michigan.gov/egle/-/media/Project/Websites/egle/Documents/Programs/AQD/State-Implementation-Plan/non-attainment/Ozone-monitors-2018-20-nonattainment-area.pdf (accessed on 20 May 2022).
8. State of Michigan. Michigan Healthy Climate Plan. Available online: https://www.michigan.gov/documents/egle/Draft-MI-Healthy-Climate-Plan_745872_7.pdf (accessed on 25 January 2022).
9. U.S. Environmental Protection Agency. *Landfill Gas Emissions Model (LandGEM) Version 3.02 User's Guide*; EPA-454/R-03-004; Office of Research and Development: Washington, DC, USA, 2005.
10. Górka, M.; Bezyk, Y.; Sówka, I. Assessment of GHG interactions in the vicinity of the municipal waste landfill site—Case study. *Energies* **2021**, *14*, 8259. [CrossRef]

11. He, H.; Wu, T.; Qiu, Z.; Zhao, C.; Wang, S.; Yao, J.; Hong, J. Enhanced methane oxidation potential of landfill cover soil modified with aged refuse. *Atmosphere* **2022**, *13*, 802. [CrossRef]
12. Bogner, J.E.; Spokas, K.A.; Chanton, J.P. Seasonal greenhouse gas emissions (methane, carbon dioxide, nitrous oxide) from engineered landfills: Daily, intermediate, and final California cover soils. *J. Environ. Qual.* **2011**, *40*, 1010–1020. [CrossRef]
13. Xu, L.; Lin, X.; Amen, J.; Welding, K.; McDermitt, D. Impact of changes in barometric pressure on landfill methane emission. *Glob. Biogeochem. Cycles* **2014**, *28*, 679–695. [CrossRef]
14. Jafari, N.H.; Stark, T.D.; Thalhamer, T. Progression of elevated temperatures in municipal solid waste landfills. *J. Geotech. Geoenviron. Eng.* **2017**, *143*, 05017004. [CrossRef]
15. Reinhart, D.; Joslyn, R.; Emrich, C.T. Characterization of Florida, U.S. landfills with elevated temperatures. *Waste Manag.* **2020**, *118*, 55–61. [CrossRef]
16. Schupp, S.; De la Cruz, F.B.; Cheng, Q.; Call, D.F.; Barlaz, M.A. Evaluation of the temperature range for biological activity in landfills experiencing elevated temperatures. *ACS EST Eng.* **2021**, *1*, 216–227. [CrossRef]
17. Monster, J.; Kjeldsen, P.; Scheutz, C. Methodologies for measuring fugitive methane emissions from landfills—A review. *Waste Manag.* **2019**, *87*, 835–859. [CrossRef] [PubMed]
18. Shah, A.; Allen, G.; Pitt, J.R.; Ricketts, H.; Williams, P.I.; Helmore, J.; Finlayson, A.; Robinson, R.; Kabbabe, K.; Hollingsworth, P.; et al. A near-field Gaussian plume inversion flux quantification method, applied to unmanned aerial vehicle sampling. *Atmosphere* **2019**, *10*, 396. [CrossRef]
19. Michigan-Ontario Ozone Source Experiment (MOOSE). Available online: https://www-air.larc.nasa.gov/missions/moose/index.html (accessed on 26 January 2022).
20. State of Michigan. Annual Reports of Solid Waste Landfilled in Michigan. Available online: https://www.michigan.gov/egle/about/organization/materials-management/solid-waste/solid-waste-disposal-areas/annual-reports-of-solid-waste-landfilled-in-michigan (accessed on 17 May 2022).
21. Xia, T.; Catalan, J.; Hu, C.; Batterman, S. Development of a mobile platform for monitoring gaseous, particulate and greenhouse gas (GHG) pollutants. *Environ. Monit. Assess.* **2021**, *193*, 7. [CrossRef] [PubMed]
22. U.S. Environmental Protection Agency. *AERMOD: Description of Model Formulation*; EPA-600/R-05/047; Office of Air Quality Planning and Standards: Research Triangle Park, NC, USA, 2004.
23. Lan, X.; Talbot, R.; Laine, P.; Torres, A. Characterizing fugitive methane emissions in the Barnett Shale area using a mobile laboratory. *Environ. Sci. Technol.* **2015**, *49*, 8139–8146. [CrossRef]
24. Olaguer, E.P.; Robinson, A.; Kilmer, S.; Haywood, J.; Lehner, D. Ethylene oxide exposure attribution and emissions quantification based on ambient air measurements near a sterilization facility. *Int. J. Environ. Res. Public Health* **2019**, *17*, 42. [CrossRef]
25. Figueroa, V.K.; Mackie, K.R.; Guarriello, N.; Cooper, C.D. A robust method for estimating landfill methane emissions. *J. Air Waste Manag. Assoc.* **2009**, *59*, 925–935. [CrossRef]
26. U.S. Environmental Protection Agency. *User's Guide for AERSURFACE Tool*; EPA-454/B-20-008; Office of Air Quality Planning and Standards: Research Triangle Park, NC, USA, 2020.
27. Shah, A.; Pitt, J.R.; Ricketts, H.; Leen, J.B.; Williams, P.I.; Kabbabe, K.; Gallagher, M.W.; Allen, G. Testing the near-field Gaussian plume inversion flux quantification technique using unmanned aerial vehicle sampling. *Atmos. Meas. Tech.* **2020**, *13*, 1467–1484. [CrossRef]
28. Carbon Mapper: Accelerating Local Climate Action, Globally. Available online: https://carbonmapper.org (accessed on 26 January 2022).
29. Galfalk, M.; Paledal, S.N.; Bastviken, D. Sensitive drone mapping of methane emissions without the need for supplementary ground-based measurements. *ACS Earth Space Chem.* **2021**, *5*, 2668–2676. [CrossRef]
30. Corbett, A.; Smith, B. A Study of a miniature TDLAS system onboard two unmanned aircraft to independently quantify methane emissions from oil and gas production assets and other industrial emitters. *Atmosphere* **2022**, *13*, 804. [CrossRef]
31. Ali, N.B.H.; Abichou, T.; Green, R. Comparing estimates of fugitive landfill methane emissions using inverse plume modeling obtained with Surface Emission Monitoring (SEM), Drone Emission Monitoring (DEM), and Downwind Plume Emission Monitoring (DWPEM). *J. Air Waste Manag. Assoc.* **2020**, *70*, 410–424.
32. Kormi, T.; Ali, N.B.H.; Abichou, T.; Green, R. Estimation of landfill methane emissions using stochastic search methods. *Atmos. Pollut. Res.* **2017**, *8*, 597–605. [CrossRef]
33. Pasquill, F.; Smith, F.B. *Atmospheric Diffusion*; Ellis Harwood: Chichester, UK, 1983.
34. Olaguer, E.P.; Stutz, J.; Erickson, M.H.; Hurlock, S.C.; Cheung, R.; Tsai, C.; Colosimo, S.F.; Festa, J.; Wijesinghe, A.; Neish, B.S. Real time measurement of transient event emissions of air toxics by tomographic remote sensing in tandem with mobile monitoring. *Atmos. Environ.* **2017**, *150*, 220–228. [CrossRef]
35. United Nations. COP26: Together for Our Planet. Available online: https://www.un.org/en/climatechange/cop26 (accessed on 30 May 2022).